Effects of postgrowth annealing treatment on the photoluminescence of zinc oxide nanorods

D. Wang, H. W. Seo, C.-C. Tin, M. J. Bozack, J. R. Williams, and M. Park[a)]
Department of Physics, Auburn University, Auburn, Alabama 36849

N. Sathitsuksanoh
Department of Chemical Engineering, Auburn University, Auburn, Alabama 36849

An-jen Cheng and Y. H. Tzeng
Department of Electrical and Computer Engineering, Auburn University, Auburn, Alabama 36849

(Received 24 October 2005; accepted 2 March 2006; published online 5 June 2006)

Postgrowth annealing was carried out to investigate the photoluminescence of zinc oxide (ZnO) nanorods synthesized using a thermal chemical vapor deposition method. The observed change in photoluminescence after the annealing processes strongly suggests that positively charged impurity ions or interstitial Zn ions are the recombination centers for green luminescence observed in the present sample. A model based on the interplay between the band bending at the surface and the migration of positively charged impurity ions or Zn ions was proposed, which satisfactorily explains the observed photoluminescence. © *2006 American Institute of Physics*. [DOI: 10.1063/1.2200593]

INTRODUCTION

The large band gap of 3.37 eV and an exciton binding energy of 60 meV make ZnO a promising material for optoelectronic applications. In addition, a one-dimensional ZnO such as a nanowire/rod exhibits interesting properties due to the quantum confinement effect and/or its very large surface to volume ratio. The luminescence of ZnO exhibits a band edge ultraviolet (UV) emission peak and a broad visible emission band related to deep level defects. The mechanism of the defect related electron-hole recombination process in ZnO has been intensively investigated, and yet it still remains a controversial subject.

Among the different mechanisms proposed to explain the visible luminescence, oxygen vacancies (V_O) have been widely considered as the most probable candidate, although no consensus could be reached regarding the charge state of the oxygen vacancy, i.e., singly ionized[1] or doubly ionized oxygen vacancy.[2] Oxygen annealing was usually employed to modify the level of oxygen deficiency in ZnO. However, contradictory results regarding the effect of annealing on the luminescence property of ZnO have been reported. In some experiments,[3–5] oxygen annealing has enhanced the intensity of the visible luminescence band and has reduced the intensity of the band edge UV luminescence band. However, in some other experiments, the exact opposite trend was observed.[6,7] It was also found that the change in relative intensities of the visible and UV luminescence band depends on the annealing temperature.[8,9] The different growth methods and postgrowth treatments result in different surface conditions. The concentration and spatial distribution of intrinsic or extrinsic defects also vary among samples. When comparing such photoluminescence data, caution needs to be exercised since all of the above mentioned factors can contribute to the characteristics of photoluminescence (PL).

In this work, postgrowth annealing was carried out to investigate the mechanism governing the visible luminescence in ZnO nanorods synthesized using a thermal chemical vapor deposition (CVD) method.

EXPERIMENT

The ZnO nanorods were grown on Si(100) substrates at 550 °C using a thermal CVD. The Zn powder (99.998%, Aldrich) was placed in an Al_2O_3 boat located inside the quartz tube reactor. Argon was used as a carrier gas. The residual oxygen in the reactor tube and/or in the Ar gas was exploited as an oxygen source.

Room temperature photoluminescence spectra were collected using a Jobin-Yvon spectrometer with a thermoelectrically cooled charge coupled device (CCD) detector. For excitation, the 325 nm (20 mW) line of a He–Cd laser (Kimmon Electric) was used. All PL spectra were collected by using the same settings. Special care was taken to ensure that the same location in the sample was probed when collecting PL.

RESULTS AND DISCUSSION

Figure 1 shows a scanning electron micrograph (SEM) of the as-grown ZnO nanorods. It can be seen that the majority of the nanorods have a diameter between 100 and 200 nm and a length of several micrometers; a few nanorods that have diameters smaller than 50 nm can also be found. The morphological and size distribution of the nanorods was fairly uniform across the sample. The sample was cut into three pieces (labeled as sample A, B, and C), and these samples were subject to different annealing/oxidation processes.

The Raman spectrum (Fig. 2) shows a strong and very sharp E_2 mode peak, which is an indication of long phonon

[a)]Author to whom correspondence should be addressed; electronic mail: park@physics.auburn.edu

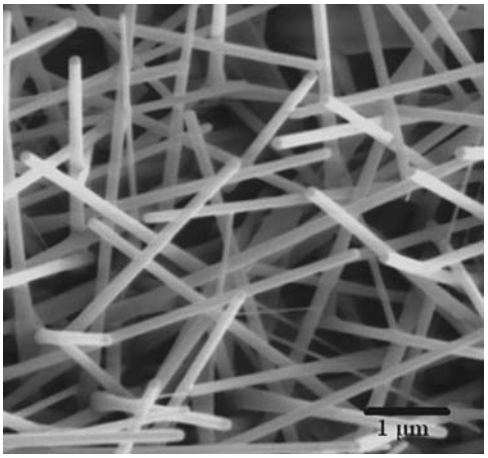

FIG. 1. SEM image of the as-grown ZnO nanorods (image size; 6×6 μm^2).

lifetime and high crystal quality. Before the annealing process, room temperature photoluminescence (PL) spectrum was collected (The spectrum from the unannealed sample are shown in Figs. 3 and 4.) As can be seen from the spectrum, the near-band-edge (NBE) peak and the green luminescence (GL) band are located at about 3.2 and 2.5 eV, respectively. No other obvious visible luminescence could be identified from the PL spectrum. The ratio of the integrated intensity of the NBE to that of the GL (I_{UV}/I_{Vis}) is 0.4.

Sample A was annealed in an oxidation furnace under flowing oxygen at 400 °C for 1 h. The PL spectrum of sample A collected after the oxygen annealing did not exhibit any changes.

The oxygen annealing of sample B was carried out at 800 °C for 1 h. The PL spectrum of sample B collected just after the oxygen annealing is shown in Fig. 3. The intensity of GL was enhanced and that of NBE was greatly reduced, decreasing I_{UV}/I_{Vis} to 0.023. Sample B was then annealed in a vacuum at 800 °C for 1 h after the annealing chamber was evacuated. After this subsequent vacuum annealing, the original PL spectrum (Fig. 3) was recovered, increasing I_{UV}/I_{Vis} to 0.42.

To make sure that the observed change in PL spectrum after oxygen annealing is related to the presence of oxygen, sample C was annealed in a vacuum at 800 °C for 1 h. The

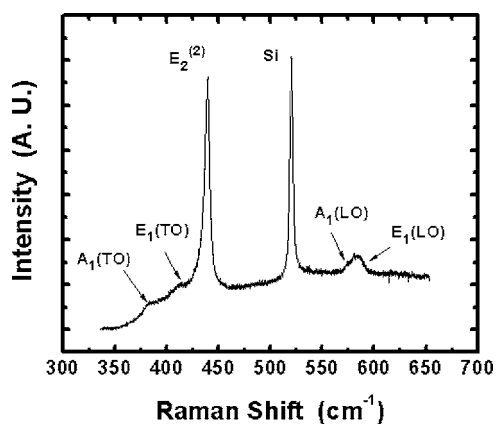

FIG. 2. Raman spectrum of the as-grown ZnO nanorods.

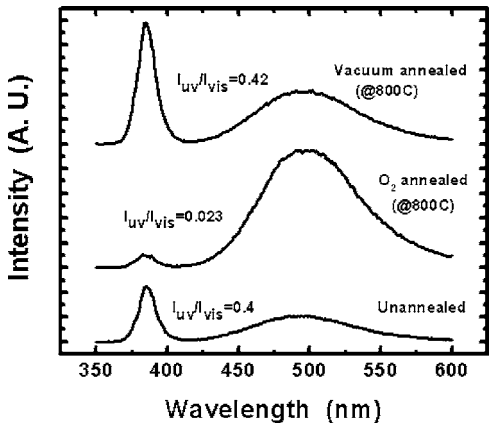

FIG. 3. PL spectra of the ZnO nanorods (sample B) collected before annealing, after O_2 annealing, and after subsequent vacuum annealing.

PL spectrum (Fig. 4) collected just after the vacuum annealing is similar to that of the as-grown sample but with an even greater I_{UV}/I_{Vis} of 0.9. Then, sample C was left in the oxidation furnace under oxygen flow at room temperature for two days. The PL spectrum (Fig. 4) collected after the oxygen exposure is similar to that of the oxidized sample B and I_{UV}/I_{Vis} was reduced to 0.077.

To make sure that the annealing condition used in this work does modify the level of oxygen deficiency in ZnO, two ZnO bulk crystals (MTI Corp.) were annealed along with sample B and sample C, respectively. After annealing, the electrical resistivities of the ZnO bulk crystals were measured. It was found that the resistivity of the oxygen annealed bulk crystal (annealed along with sample B) was increased by more than one order of magnitude than that of the unannealed bulk crystal, while the resistivity of the vacuum annealed bulk crystal (annealed along with sample C) was decreased by more than two orders of magnitude than that of the unannealed sample. The excess zinc content or higher level oxygen deficiency in the vacuum annealed ZnO gives rise to the lower resistivity. The same behavior of electrical resistivity dependence on the level of oxygen deficiency has been reported for ZnO grown or annealed in different ambient gas conditions.[10,11] Despite the obvious changes of oxy-

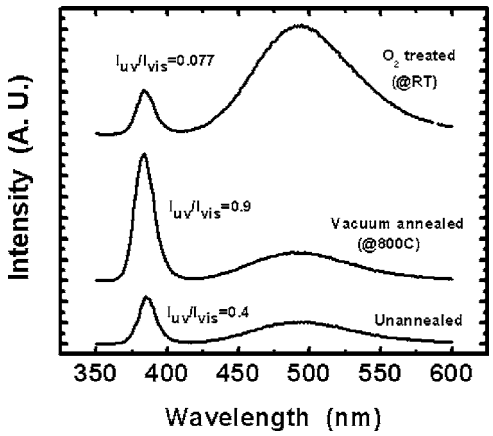

FIG. 4. PL spectra of the ZnO nanorods (sample C) collected before annealing, after vacuum annealing, and after the subsequent exposure to oxygen ambient for two days.

gen composition by the annealing processes, our experiments, as well as those performed by other groups[3–5] that employed various annealing conditions, have shown the opposite trend in PL to what is predicted by the V_O model.

Although the detailed nature of the recombination center that is responsible for GL is still under debate, it is generally agreed that GL is a surface related process. Both the comparative study of nanowires with different surface to volume ratios[12] and the direct imaging using cathodoluminescence microscopy[13] have shown that the GL process is localized at the surface of the nanowires. Li *et al.* has found that the GL can be suppressed by coating the ZnO nanostructure with surfactant.[14] It was also found that surface passivation by coating ZnO thin film with alkali halide[15] or a dielectric layer[16] can suppress GL and enhance NBE.

It is well known that the chemisorption of oxygen at the ZnO surface causes an upward band bending by capturing electrons in a region near the surface.[17] This adsorption process can occur in the air at room temperature, producing upward band bending in the as-grown ZnO. Upon excitation, the photogenerated electrons and holes near the surface are swept to the opposite directions across the depletion region, thus greatly reducing their chances of recombination through excitonic processes. Upon arriving at the surface, holes can be captured by the adsorbed oxygen ion, followed by transforming into physisorbed state. The physisorbed oxygen is less stable and is prone to be desorbed from the surface, thus reducing the thickness of the depletion layer. This phenomenological model has been also utilized to explain the UV illumination enhanced PL effect in ZnO thin film.[18]

The depth of the surface recombination layer was estimated to be 30 nm.[9] Muth *et al.*[19] have measured the absorption coefficient of ZnO, and have found a large absorption coefficient of $\sim 160\,000\ \mathrm{cm}^{-1}$ at 325 nm, which corresponds to a penetration depth of ~ 60 nm. Since a substantial number of photogenerated electro-hole pairs fall within the surface depletion region, any change of the depletion layer will have a significant impact on the overall characteristics of luminescence. A direct consequence is the effect of ambient gas on the luminescence. The more the chemisorption of oxygen occurs at ZnO surface, the fewer holes are left in the bulk to recombine with electrons through excitonic processes. Instead, more holes will be trapped near the surface where they can recombine nonradiatively with electrons via surface states or radiatively via deep level defect states to generate GL.[2]

Lagowski *et al.*[17] found that the 0.72 eV thermal activation energy needed for the charge transfer through the surface potential barrier is the major limiting factor for determining the chemisorption rate. They found that the rate of charge transfer increases linearly with increasing oxygen pressure and exponentially with increasing temperature. In our experiment, annealing at an elevated temperature in an oxygen ambient greatly increases the number of chemisorbed oxygen, leading to the enhanced GL. On the other hand, vacuum annealing removes the excess chemisorbed oxygen and recovers the original PL.

Even with the formation of the depletion layer, the GL still cannot occur without enough deep level recombination centers that exist near the surface. Had V_O been the dominant recombination center for GL, we would have seen a decrease of GL after the oxygen annealing since the V_O had been removed. The same rationale can be applied to the vacuum annealing regardless of the change in the band bending. It is clear that something other than V_O is playing a dominant role as the recombination center for GL.

Cu impurity has also been considered as a recombination center that can lead to GL. Garces *et al.*[20] concluded that the broad structureless GL at 500 nm is due to donor-acceptor pair (DAP) recombination between an electron bound to a shallow donor and a hole loosely bound to the Cu^+. At a high enough temperature impurity ions can drift along the direction of an external electric field. Korsunska *et al.*[21] have reported the increase of GL intensity near the cathode and decrease near the anode when an external electric field was applied across a ZnO single crystal at 600–700 °C. They attribute the change in GL to the electrodiffusion of Zn interstitial (Zn_i). The same group also reported that Cu impurity in CdS drifted from anode to cathode in the form of Cu_i^+ under the influence of external electric field.[22]

We found that the observed change in PL after each annealing process can be explained by a model based on both the band bending and the migration of impurities. We believe that two major processes occur during the oxygen annealing: (1) the increase of the number of chemisorption of oxygen at the surface, followed by band bending at the near surface region, and (2) the migration of positively charged impurity ions or Zn_i to the surface under the influence of the built-in electric field in the depletion region. Since a substantial amount of photogenerated holes are swept to the surface, the segregation of impurity ions or Zn_i in the surface region increases the chance of photogenerated holes being trapped by them. Photogenerated electrons transported to the surface region can then recombine with the trapped holes. Those holes not trapped by impurity ions are then captured by the adsorbed oxygen or other surface states, causing the desorption of oxygen or nonradiative recombination with photogenerated electrons. Due to the interception of impurity ions or Zn_i, fewer holes can reach the surface oxygen to cause the desorption. Thus, the segregated impurity ions or Zn_i can act as a trap to reduce the number of photogenerated holes reaching the chemisorbed oxygen, which is also in favor of GL.

Let us now look at the two processes occurring during the vacuum annealing: (1) desorption of surface oxygen and a lesser degree of band bending when compared with the unannealed sample, and (2) migration of impurity ions or Zn_i, which is similar to what oxygen annealing will produce but to a lesser extent. After the vacuum annealing, the width of the depletion layer is greatly reduced and the band becomes flat, resulting in a strong NBE and a weak GL in PL (Fig. 4). After the subsequent exposure to oxygen ambient for two days, the surface will be covered with oxygen again, followed by band bending. This readsorption of oxygen decreases NBE and increases GL, as is shown in Fig. 4. It is interesting to note that the PL of sample C collected after the exposure to oxygen ambient is more similar to that of sample B after oxygen annealing, and shows more prominent GL

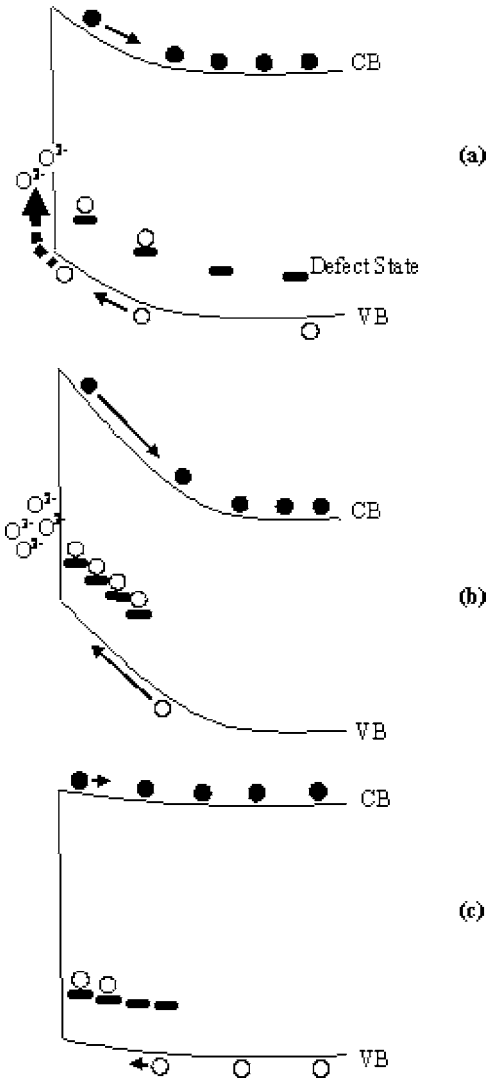

FIG. 5. Schematics of the energy band diagram (not scaled) that illustrate the band bending and dynamics of the photogenerated electron-hole pairs near the surface of sample B when it was illuminated by above band-gap excitation at three different stages: (a) as grown, (b) after oxygen annealing, and (c) after subsequent vacuum annealing. Only doubly ionized oxygen ions O^{2-} are used for illustration. The capturing process of photogenerated holes by chemisorbed oxygen ions is depicted by the broken arrow.

when compared with the original PL of the as-grown sample. This is due to the fact that the redistribution of the defect states creates more recombination centers near the surface. Therefore, the result of the vacuum annealing and the subsequent exposure in oxygen is similar to that obtained by just a single oxygen annealing step. Finally, when the oxygen annealed sample B was subsequently vacuum annealed, its PL was recovered to the original PL. This change, however, is solely due to the desorption of oxygen.

The band bending and the dynamics of photogenerated electron-hole pairs are illustrated in Fig. 5 for sample B when it undergoes three different stages: as grown, after oxygen annealing, and after subsequent vacuum annealing. A similar set of energy band diagrams can be given to sample C by switching the order of Figs. 5(b) and 5(c).

At a low annealing temperature of 400 °C, adsorption and desorption of oxygen still occur at a lower rate, but significant diffusion of impurities or Zn_i in ZnO requires higher temperature as dictated by the temperature dependence of the diffusion coefficient; $D=D_0\exp(-E_A/k_BT)$. For Zn_i diffusion in ZnO, $D_0=1.7\times10^2$ cm^2/s, and $E_A=3.3$ eV.[23] For Cu diffusion in ZnO, $D_0=2\times10^7$ cm^2/s and $E_A=4.8$ eV,[23] thus Cu diffusion requires even higher temperature than Zn_i diffusion due to a larger activation energy E_A. The high temperature needed for the diffusion of impurity or Zn_i explains the insignificant change in the PL of sample A (annealed at 400 °C).

As for the identity of this defect state, Cu^+ seems like a good candidate, but the source of Cu contamination in the growth process cannot be determined. A Zn_i related complex has also been suggested as the recombination center of GL,[21] but it was shown[24] that the interstitial Zn^+ diffuses to the surface to form $[Zn^{2+}-O^{2-}]$ surface pair, which emits UV light. Radiative transition may happen from conduction band or shallow donors to Zn vacancy acceptor at around 2.6 eV,[25] but V_{Zn} is negatively charged in its stable state. Therefore, the upward band bending will drive V_{Zn} away from the surface. More information is needed to identify this deep level defect state.

Unlike ZnO nanostructure, the influence of postdeposition annealing on ZnO films is also related to the change in the microstructure of the films. According to the structure zone model,[26] a process of coalescence and major grain growth result in a porous and cracked structure in the films when annealed at an elevated temperature.[8,27] On the other hand, ZnO nanostructures usually exhibit a single crystal structure and have a small dimension. Therefore, structural defects can easily migrate out, and the localized strain can be relieved by bending during the growth.

CONCLUSIONS

We have carried out oxygen and vacuum annealing experiment to study the mechanism of GL of ZnO nanorods synthesized by thermal CVD. Our experiment results reveal that V_O is not the dominant recombination center for GL observed in the present sample. A model based on the interplay between the band bending at the surface and the migration of positively charged impurity ions or Zn_i was proposed, which satisfactorily explains the observed change in PL after each annealing process. Its sensitivity to the oxygen ambient may be a useful property for the ZnO nanorod to be used in oxygen gas sensing applications.

ACKNOWLEDGMENTS

The authors would like to thank the Office of the Associate Provost and Vice President for Research (OVPR) at Auburn University for partial support through the Competitive Research Grant. Portions of the work were also supported by Auburn University Detection and Food Safety Center (AUDFS) through a United States Department of Agriculture (USDA) grant under Contract No. 2005 3439415674A.

[1] K. Vanheusden, W. L. Warren, C. H. Seager, D. R. Tallant, J. A. Voigt, and B. E. Gnade, J. Appl. Phys. **79**, 7983 (1996); K. Vanheusden, C. H. Seager, W. L. Warren, D. R. Tallant, and J. A. Voigt, Appl. Phys. Lett. **68**, 403 (1996).

[2]A. van Dijken, E. A. Meulenkamp, D. Vanmaekelberg, and A. Meijerink, J. Phys. Chem. B **104**, 1715 (2000).
[3]T. Sekiguchi, N. Ohashi, and Y. Terada, Jpn. J. Appl. Phys., Part 2 **36**, L289 (1997).
[4]X. Liu, X. H. Wu, H. Cao, and R. P. H. Chang, J. Appl. Phys. **95**, 3141 (2004).
[5]W. S. Shi, O. Agyeman, and C. N. Xu, J. Appl. Phys. **91**, 5640 (2002).
[6]B. X. Lin, Z. X. Fu, Y. B. Jia, and G. H. Liao, J. Electrochem. Soc. **148**, G110 (2001).
[7]M. Anpo and Y. Kubokawa, J. Phys. Chem. **88**, 5556 (1984).
[8]S. H. Bae, S. Y. Lee, H. Y. Kim, and S. Im, Opt. Mater. (Amsterdam, Neth.) **17**, 327 (2001).
[9]Y. G. Wang, S. P. Lau, H. W. Lee, S. F. Yu, B. K. Tay, X. H. Zhang, and H. H. Hng, J. Appl. Phys. **94**, 354 (2003).
[10]T. Inukai, M. Matsuoka, and K. Ono, Thin Solid Films **257**, 22 (1995).
[11]J. D. Ye *et al.*, J. Appl. Phys. **96**, 5308 (2004).
[12]I. Shalish, H. Temkin, and V. Narayannamurti, Phys. Rev. B **69**, 245401 (2004).
[13]T. Nobis, E. M. Kaidashev, A. Rahm, M. Lorenz, J. Lenzner, and M. Grundmann, Nano Lett. **4**, 797 (2004).
[14]D. Li, Y. H. Leung, A. B. Djurišić, Z. T. Liu, M. H. Xie, S. L. Shi, S. J. Xu, and W. K. Chan, Appl. Phys. Lett. **85**, 1601 (2004).
[15]Y. Harada and S. Hashimoto, Phys. Rev. B **68**, 045421 (2003).
[16]K. C. Hui, H. C. Ong, P. F. Lee, and J. Y. Dai, Appl. Phys. Lett. **86**, 152116 (2005).
[17]J. Lagowski, E. S. Sproles, Jr., and H. C. Gatos, J. Appl. Phys. **48**, 3566 (1977).
[18]Chunming Jin, dissertation, North Carolina State University, 2003.
[19]J. F. Muth, R. M. Kolbas, A. K. Sharma, S. Oktyabrsky, and J. Narayan, J. Appl. Phys. **85**, 7884 (1999).
[20]N. Y. Garces, L. Wang, L. Bai, N. C. Giles, L. E. Halliburton, and G. Cantwell, Appl. Phys. Lett. **81**, 622 (2002).
[21]N. E. Korsunska, L. V. Borkovska, B. M. Bulakh, L. Yu. Khomenkova, V. I. Kushnirenko, and I. V. Markevich, J. Lumin. **102–103**, 733 (2003).
[22]N. E. Korsunska, I. V. Markevich, L. V. Borkovska, L. Yu. Khomenkova, M. K. Sheinkman, and O. Yastrubchak, Physica B **308–310**, 967 (2001).
[23]K. H. Hellwege, O. Madelung, and A. M. Hellege, *Numerical Data and Functional Relationship in Science and Technology* (Springer-Verlag, New York, 1987).
[24]R. J. Kokes, J. Phys. Chem. **66**, 99 (1962).
[25]A. F. Kohan, G. Ceder, D. Morgan, and C. G. Van de Walle, Phys. Rev. B **61**, 15019 (2000).
[26]V. Gupta and A. Mansingh, J. Appl. Phys. **80**, 1063 (1996).
[27]Z. B. Fang, Z. J. Yan, Y. S. Tan, X. Q. Liu, and Y. Y. Wang, Appl. Surf. Sci. **241**, 303 (2005).